Applied Physics Letters

RESEARCH ARTICLE | MARCH 06 2023

Implementation of SNS thermometers into molecular devices for cryogenic thermoelectric experiments

Serhii Volosheniuk; Damian Bouwmeester; Chunwei Hsu; ... et. al

Appl. Phys. Lett. 122, 103501 (2023)
https://doi.org/10.1063/5.0137392

Applied Physics Letters ARTICLE scitation.org/journal/apl

Implementation of SNS thermometers into molecular devices for cryogenic thermoelectric experiments

Cite as: Appl. Phys. Lett. **122**, 103501 (2023); doi: 10.1063/5.0137392
Submitted: 2 December 2022 · Accepted: 20 February 2023 ·
Published Online: 6 March 2023

Serhii Volosheniuk,[1] Damian Bouwmeester,[1] Chunwei Hsu,[1] H. S. J. van der Zant,[1] and Pascal Gehring[2,a)]

AFFILIATIONS

[1]Kavli Institute of Nanoscience, Delft University of Technology, Lorentzweg 1, 2628 CJ Delft, The Netherlands
[2]IMCN/NAPS, Université Catholique de Louvain (UCLouvain), 1348 Louvain-la-Neuve, Belgium

[a)]Author to whom correspondence should be addressed: pascal.gehring@uclouvain.be

ABSTRACT

Thermocurrent flowing through a single-molecule device contains valuable information about the quantum properties of the molecular structure and, in particular, on its electronic and phononic excitation spectra and entropy. Furthermore, accessing the thermoelectric heat-to-charge conversion efficiency experimentally can help to select suitable molecules for future energy conversion devices, which—predicted by theoretical studies—could reach unprecedented efficiencies. However, one of the major challenges in quantifying thermocurrents in nanoscale devices is to determine the exact temperature bias applied to the junction. In this work, we have incorporated a superconductor–normal metal–superconductor Josephson junction thermometer into a single-molecule device. The critical current of the Josephson junction depends accurately on minute changes in the electronic temperature in a wide temperature range from 100 mK to 1.6 K. Thus, we present a device architecture which can enable thermoelectric experiments on single molecules down to millikelvin temperatures with high precision.

Thermoelectric effects, i.e., the conversion between heat and charge currents, have received renewed interest from the nanoelectronics community[1,2] and, in particular, in the field of single-molecule electronics.[3,4] Recent studies[5–9] show that thermoelectric measurements at cryogenic temperatures contain important information about the physical and quantum-thermodynamic properties of nanoscale and molecular systems, which are hard to access with conventional transport experiments. Furthermore, according to theoretical predictions, molecular devices could achieve a very high dimensionless figure of merit[10] ZT—a quantity that is a measure for the heat-to-charge conversion efficiency. While the highest observed ZT of inorganic materials is currently only[11] about 5–6, the predicted ZT of molecular heat engines could reach values of $\approx$100, which would result in efficiencies close to the Carnot efficiency limit.[12] This efficiency could be even further enhanced at cryogenic temperature.[13] However, to quantify thermoelectric effects, it is primordial to know the exact temperature drop across a molecular junction. This is, in particular, challenging at cryogenic temperature because most thermometers used so far are metal-based resistive sensors with low sensitivity at $T < 20$ K. This work fills this gap by developing a superconducting thermometer, which is sensitive down to mK temperature, and by implementing this thermometer into an electromigrated break junction (EMBJ) device.

Different types of low-temperature thermometry approaches have been explored in the literature, including Johnson Noise thermometry,[14] Coulomb Blockade thermometry,[15] and Hybrid Tunnel Junction thermometry.[16] In this article, we focus on superconductor–normal metal–superconductor (SNS) thermometers because of their excellent properties: low impedance, high sensitivity at low temperatures, and a negligible access resistance.[17] Furthermore, they can be easily implemented into molecular junctions: To this end, we further improve our single-molecule thermoelectric junctions,[18] by contacting the source and drain gold contacts with two superconductors, forming a local SNS junction. By measuring the critical current over this SNS junction, the temperature can be extracted. In this manner, the contacts can be simultaneously used for thermometry and transport measurements. Here, we use a molybdenum rhenium (MoRe) superconductor, for its high critical temperature of 8.7 K (with a zero-temperature superconducting gap of about $\Delta \approx 1.8 k_B T_C \approx 1.3$ meV).

The fabrication procedure of the devices on Si wafers with a 285 nm layer of SiO_2 oxide is illustrated in Figs. 1(a)–1(d).

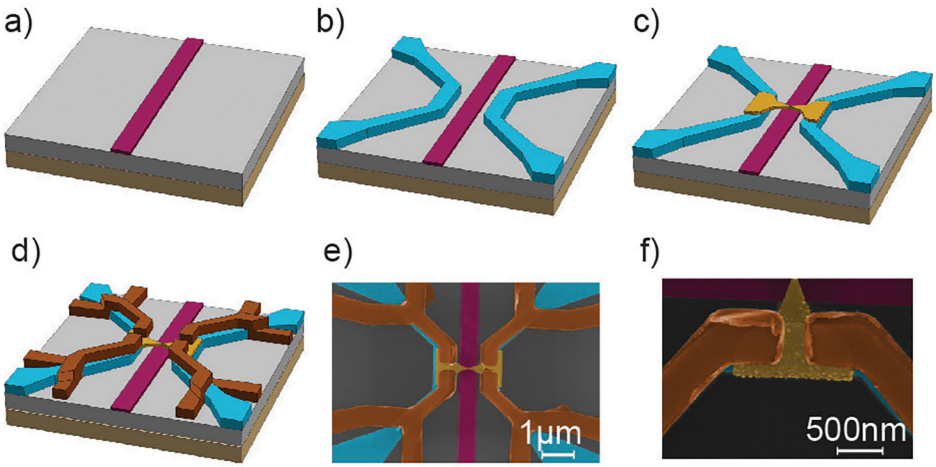

FIG. 1. (a)–(d) Fabrication process overview. (a) Electron beam (E-beam) deposition of the local back gate electrode (purple). (b) Deposition of sample heaters (blue). (c) Deposition of 13 nm thick gold bridge (yellow). (d) Metal sputtering of superconducting contacts which act as source/drain connections and thermometers. (e) and (f) False-colored scanning-electron microscopy (SEM) images of the fabricated sample. (e) False-colored SEM picture of the thermopower device and (f) of the MoRe/Au/MoRe junction; purple: gate electrode; blue: heaters; yellow: gold bridge; and brown: MoRe contacts.

First [Fig. 1(a)], the local gate was made by depositing a 1 nm thick adhesion layer of titanium (Ti) and a 7 nm thick layer of palladium (Pd) by standard electron-beam lithography and metal evaporation. This gate thickness is chosen to decrease the heat transport from source to drain.[18] Then, the heater was fabricated by depositing 3 nm of Ti and 27 nm of Pd [Fig. 1(b)]. Subsequently, 10 nm Al_2O_3 was deposited by atomic layer deposition. The aluminum oxide forms the insulating layer between the heater and the electrical contacts and acts as the dielectric of the local gate. Afterward, the 13 nm thick Au bridge was made [see Fig. 1(c)]. To get a high-quality gold bridge, the deposition rate during evaporation was kept low (0.5 A/s) and a high vacuum around 10^{-8} mbar was used. In the last step, the 100 nm thick MoRe contacts were created by electron-beam lithography, metal sputtering, and liftoff [Fig. 1(d)].

False-colored scanning electron microscope (SEM) images of the final device together with a zoom-in of an individual Josephson junction are shown in Figs. 1(e) and 1(f). The spacing between the superconducting contacts varies and is 253 nm on one side of the gold bridge (thermometer A) and 247 nm on the other side (thermometer B), in the device shown here.

To calibrate the thermometers, devices were cooled down to 100 mK in a dilution refrigerator. A four-point measurement scheme was applied, where a DC (I_{JJ}) was biased over the junction and the voltage response (V_{JJ}) was simultaneously recorded. A typical DC–voltage characteristic at 100 mK for thermometer A is shown in Fig. 2(a). In the low-current regime, the gold bridge between the two superconductors is proximitized and the Cooper pairs can move from one superconductor to the other without dissipation, forming an Andreev bound state.[19] At a certain current level—i.e., at the switching current (I_{SW})—the gold weak link changes its state from superconducting to normal, resulting in a voltage increase in the current–voltage (I–V) characteristic. From the slope of the I–V characteristic at $I > I_{SW}$, the normal resistance of the gold weak link is calculated and the diffusion coefficient of the electrons in this region is estimated. When ramping the current back, the gold weak link becomes superconducting again at the retrapping current (I_R). This current value typically differs from I_{SW}, which has been explained by capacitive effects in the junction[20] or by heating of the electrons in the normal conducting junction during current sweeping.[21] Since the geometrical capacitance of the junctions used in this work is not sufficiently large to explain the existence of the retrapping current, we attribute the observed hysteresis to heating.

Importantly, the switching to the superconducting state with increasing current bias is a stochastic process,[22] so several I–V curves need to be recorded and a mean value of I_{SW} is calculated. To this end, the critical current was measured with an AC technique[23] [see Fig. 2(b)]. In a typical measurement, the junction is biased with a 300 Hz triangular AC from −20 to 87 μA. At these settings, gold stays in the normal state only for a short time, preventing the system from heating. Also, the offset is chosen to ensure that the junction stays proximitized in the negative current part and can relax to the base temperature. Using this approach, in a typical experiment, we recorded 3000 measurements of switching events with a current resolution of about 0.07 μA.

Using the AC measurement technique, it is possible to measure I_{SW} at different base temperatures and calibrate the thermometers in the device. The I_{SW} histograms for thermometer A are shown in Fig. 2(c). It can be seen that the switching current is very sensitive to the sample temperature and decreases from 80 μA at 150 mK to 61 μA at 750 mK. We also note an asymmetry in the switching current distributions. Such asymmetry has been observed before[24] and attributed to thermal fluctuations. The stochasticity of switching current is dominated by quantum noise at temperatures below the Thouless energy, while thermal fluctuations become the dominating mechanism at higher temperatures (see discussion in Sec. III of the supplementary material). From the fits to the current histograms, we extract the average switching current $\langle I_{sw} \rangle$ as a function of temperature for the two thermometers (see Fig. 3). The sensitivity of the thermometers, defined as $\frac{dI_{SW}}{dT}$, in the temperature range from 100 to 750 mK is 31.5 and 42 μA/K for thermometers A and B, respectively (see Sec. II of the supplementary material for data of other thermometers and Sec. V of the supplementary material for a comparison with other Au-based SNS thermometers). These values are typical for long SNS junctions and similar to those reported for Nb–Cu–Nb SNS junctions.[25]

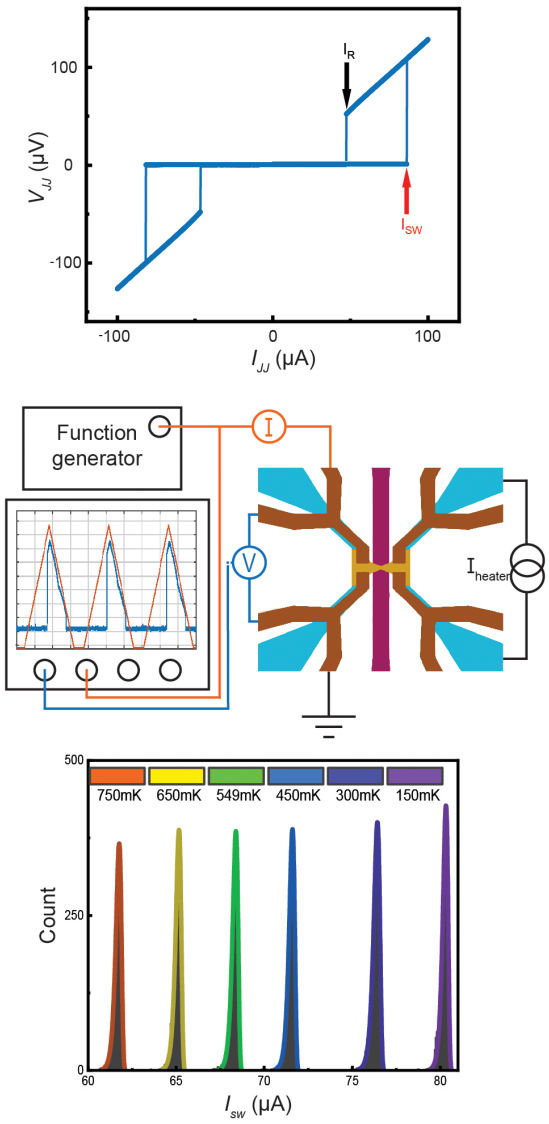

FIG. 2. (a) Voltage vs current characteristics of a MoRe/Au/MoRe junction. The current was ramped up from 0 to 100 μA, then to -100 μA and back to zero. (b) Schematic of the signal path during an AC experiment. A function generator was used to bias the superconducting thermometer with a current I and to measure the voltage drop V on the thermometer. A DC heater current I_{heat} can be applied to one of the microheaters to generate a thermal bias on the junction. (c) Histogram of stochastic switching current I_{sw} of a SNS junction at different temperatures.

Furthermore, both thermometers have a temperature resolution better than 15 mK within the investigated temperature range (see Sec. IV of the supplementary material for more details).

In the following, we discuss the temperature dependence of $\langle I_{sw} \rangle$ (see Fig. 3). In Josephson junctions, this dependence is very sensitive to the interplay between the energy scales of the proximity effect, the Thouless energy, $E_{TH} = \frac{\hbar D}{L^2}$, and the superconducting gap Δ. Here, $D = \frac{v_F l_e}{3}$ is the diffusion coefficient in the normal metal, where v_F, l_e are the Fermi velocity and the elastic mean free path of electrons,

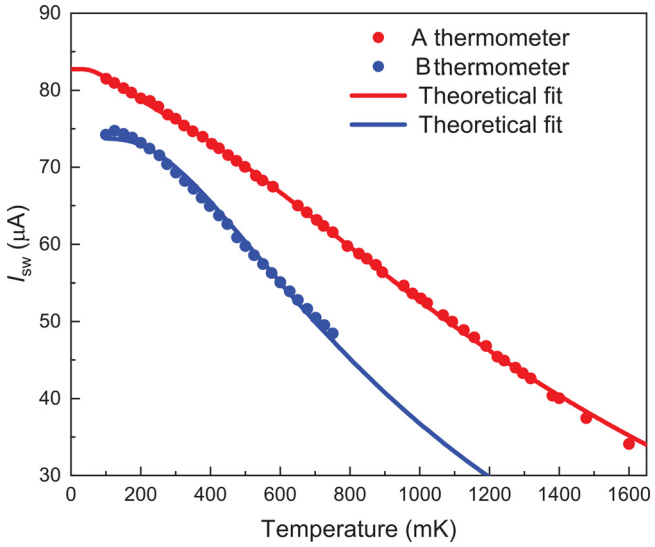

FIG. 3. Temperature dependence of the averaged switching current, $\langle I_{SW} \rangle$, for thermometers A (red) and B (blue), respectively. Theoretical fits using the Usadel equation (see the main text) are shown as solid lines.

respectively, and L is the distance between the superconducting electrodes. In the long junction limit $\Delta > E_{TH}$, the temperature dependence of I_{SW} can be described theoretically by using a quasi-classical approach based on Green's functions in imaginary space;[26,27] it requires solving the Usadel equation at all energies.[27]

We used the *usadel1* package[28] to fit the experimental data. We assumed that the interfaces between the superconductor and the normal metal are perfectly transparent and that the phase difference between the superconductors is fixed at $\phi = 1.27\pi/2$, similar to Dubos *et al.*[27] Furthermore, we fixed the normal resistance, R_N, of the junction and Δ of the superconductor to values obtained from transport measurements. The solid lines in Fig. 3 show the resulting fits where the Thouless energy and the suppression coefficient, α, which accounts for the non-ideality of the normal metal-superconductor contact, were used as fitting parameters. Details about the fitting and the resulting parameters can be found in the supplementary material. We find a suppression coefficient $\alpha \approx 0.5$, similar to the value obtained by Courtois *et.al.*[21] The Thouless energies, $E_{TH}^{FIT} = 49.4$ –87.2 μeV, obtained from the fits in Fig. 3 are close to the values determined from the transport measurements, $E_{TH}^{EXP} \approx 40$ μeV, which can be calculated as[29] $E_{TH}^{EXP} = \frac{1}{VN(E_F)} \frac{R_Q}{2\pi R_N}$, where $V = L \cdot w \cdot t$ is the volume of the gold film, $N(E_F)$ is the volumetric electronic density of states of gold at the Fermi level, and $R_Q = \frac{h}{2e^2}$ is the resistance quantum. $N(E_F)$ can be obtained from the electronic specific heat[30] $\gamma = 0.69 \times 10^{-3}$ J mol^{-1} K^{-2} and the molar volume[31] $v = 1.021 \times 10^{-5}$ m^3 mol^{-1} as[32] $N(E_F) = \frac{3\gamma}{\pi^2 k_B^2 v} = 1.73 \times 10^{28}$ eV^{-1} m^{-3}.

In summary, we implemented an SNS superconducting thermometer in a molecular thermoelectric device. MoRe was used as the superconductor, which allows to perform thermometry in a temperature range from 100 mK to 1.6 K with a high sensitivity of up to 40 μA/K. Other than previously used resistance thermometers, the SNS thermometers developed in this work directly measure the

temperature of the electronic system in the immediate proximity to the molecule. Therefore, our devices will allow us to, e.g., extract the absolute Seebeck coefficient from thermopower measurements on a molecule and will, thus, pave the way for precise investigations of molecular heat engines.

See the supplementary material for a theoretical fit to thermometer A with two parameters; results of test thermometers with different L– spacing; discussion of I_{SW} fluctuations; temperature resolution of thermometers; and comparison with other Au-based SNS junctions.

The authors acknowledge the financial support from the F.R.S.-FNRS of Belgium (FNRS-CQ-1.C044.21-SMARD, FNRS-CDR-J.0068.21-SMARD, and FNRS-MIS-F.4523.22-TopoBrain), from the Federation Wallonie-Bruxelles through the ARC Grant No. 21/26-116, and from the EU (ERC-StG-10104144-MOUNTAIN and FET-767187-QuIET). This project (No. 40007563-CONNECT) has received funding from the FWO and F.R.S.-FNRS under the Excellence of Science (EOS) programme. This work was supported by the Netherlands Organisation for Scientific Research (NWO/OCW), as a part of the Frontiers of Nanoscience program and Natuurkunde Vrije Programma's: 680.90.18.01.

AUTHOR DECLARATIONS

Conflict of Interest

The authors have no conflicts to disclose.

Author Contributions

Serhii Volosheniuk: Investigation (lead); Methodology (lead); Resources (lead); Software (equal); Validation (equal); Visualization (lead); Writing – original draft (lead); Writing – review & editing (equal). **Damian Bouwmeester:** Investigation (supporting); Software (equal); Validation (equal). **Chunwei Hsu:** Methodology (supporting); Resources (supporting); Validation (equal). **Herre S. J. van der Zant:** Supervision (equal); Writing – review & editing (equal). **Pascal Gehring:** Conceptualization (lead); Funding acquisition (equal); Supervision (equal); Writing – review & editing (equal).

DATA AVAILABILITY

The data that support the findings of this study are available from the corresponding author upon request.

REFERENCES

[1]J. P. Heremans, M. S. Dresselhaus, L. E. Bell, and D. T. Morelli, "When thermoelectrics reached the nanoscale," Nat. Nanotechnol. **8**, 471–473 (2013).
[2]A. Gemma and B. Gotsmann, "A roadmap for molecular thermoelectricity," Nat. Nanotechnol. **16**, 1299–1301 (2021).
[3]L. Rincón-García, C. Evangeli, G. Rubio-Bollinger, and N. Agraït, "Thermopower measurements in molecular junctions," Chem. Soc. Rev. **45**, 4285–4306 (2016).
[4]K. Wang, E. Meyhofer, and P. Reddy, "Thermal and thermoelectric properties of molecular junctions," Adv. Funct. Mater. **30**, 1904534 (2020).
[5]M. Josefsson, A. Svilans, A. M. Burke, E. A. Hoffmann, S. Fahlvik, C. Thelander, M. Leijnse, and H. Linke, "A quantum-dot heat engine operating close to the thermodynamic efficiency limits," Nat. Nanotechnol. **13**, 920–924 (2018).
[6]Y. Kleeorin, H. Thierschmann, H. Buhmann, A. Georges, L. W. Molenkamp, and Y. Meir, "How to measure the entropy of a mesoscopic system via thermoelectric transport," Nat. Commun. **10**, 5801 (2019).
[7]B. Dutta, D. Majidi, A. García Corral, P. A. Erdman, S. Florens, T. A. Costi, H. Courtois, and C. B. Winkelmann, "Direct probe of the Seebeck coefficient in a Kondo-correlated single-quantum-dot transistor," Nano Lett. **19**, 506–511 (2019).
[8]E. Pyurbeeva, C. Hsu, D. Vogel, C. Wegeberg, M. Mayor, H. van der Zant, J. A. Mol, and P. Gehring, "Controlling the entropy of a single-molecule junction," Nano Lett. **21**, 9715–9719 (2021).
[9]C. Hsu, T. Costi, D. Vogel, C. Wegeberg, M. Mayor, H. van der Zant, and P. Gehring, "Magnetic field universality of the Kondo effect revealed by thermocurrent spectroscopy," Phys. Rev. Lett. **128**, 147701 (2022).
[10]M. Paulsson and S. Datta, "Thermoelectric effect in molecular electronics," Phys. Rev. B **67**, 241403 (2003).
[11]B. Hinterleitner, I. Knapp, M. Poneder, Y. Shi, H. Müller, G. Eguchi, C. Eisenmenger-Sittner, M. Stöger-Pollach, Y. Kakefuda, N. Kawamoto, Q. Guo, T. Baba, T. Mori, S. Ullah, X.-Q. Chen, and E. Bauer, "Thermoelectric performance of a metastable thin-film Heusler alloy," Nature **576**, 85–90 (2019).
[12]C. M. Finch, V. M. García-Suárez, and C. J. Lambert, "Giant thermopower and figure of merit in single-molecule devices," Phys. Rev. B **79**, 033405 (2009).
[13]A. Harzheim, J. K. Sowa, J. L. Swett, G. A. D. Briggs, J. A. Mol, and P. Gehring, "Role of metallic leads and electronic degeneracies in thermoelectric power generation in quantum dots," Phys. Rev. Res. **2**, 013140 (2020).
[14]A. Casey, B. Cowan, H. Dyball, J. Li, C. Lusher, V. Maidanov, J. Nyeki, J. Saunders, and D. Shvarts, "Current-sensing noise thermometry from 4.2 K to below 1 mK using a DC squid preamplifier," Physica B **329–333**, 1556–1559 (2003).
[15]J. P. Pekola, K. P. Hirvi, J. P. Kauppinen, and M. A. Paalanen, "Thermometry by arrays of tunnel junctions," Phys. Rev. Lett. **73**, 2903–2906 (1994).
[16]J. M. Rowell and D. C. Tsui, "Hot electron temperature in INAS measured by tunneling," Phys. Rev. B **14**, 2456–2463 (1976).
[17]B. Dutta, "Energetics in metallic-island and quantum-dot based single-electron devices," Theses (Université Grenoble Alpes, 2018).
[18]P. Gehring, M. van der Star, C. Evangeli, J. J. Le Roy, L. Bogani, O. V. Kolosov, and H. S. J. van der Zant, "Efficient heating of single-molecule junctions for thermoelectric studies at cryogenic temperatures," Appl. Phys. Lett. **115**, 073103 (2019).
[19]J. A. Sauls, "Andreev bound states and their signatures," Philos. Trans. R. Soc. A **376**, 20180140 (2018).
[20]W. C. Stewart, "Current-voltage characteristics of Josephson junctions," Appl. Phys. Lett. **12**, 277 (1968).
[21]H. Courtois, M. Meschke, J. T. Peltonen, and J. P. Pekola, "Origin of hysteresis in a proximity Josephson junction," Phys. Rev. Lett. **101**, 067002 (2008).
[22]L. Angers, F. Chiodi, G. Montambaux, M. Ferrier, S. Guéron, H. Bouchiat, and J. C. Cuevas, "Proximity dc squids in the long-junction limit," Phys. Rev. B **77**, 165408 (2008).
[23]B. Dutta, D. Majidi, N. W. Talarico, N. Lo Gullo, H. Courtois, and C. B. Winkelmann, "Single-quantum-dot heat valve," Phys. Rev. Lett. **125**, 237701 (2020).
[24]K. Spahr, J. Graveline, C. Lupien, M. Aprili, and B. Reulet, "Dynamical voltage-current characteristics of SNS junctions," Phys. Rev. B. **102**, 100504(R) (2020).
[25]P. Dubos, H. Courtois, O. Buisson, and B. Pannetier, "Coherent low-energy charge transport in a diffusive S-N-S junction," Phys. Rev. Lett. **87**, 206801 (2001).
[26]W. Belzig, F. K. Wilhelm, C. Bruder, G. Schön, and A. D. Zaikin, "Quasiclassical Green's function approach to mesoscopic superconductivity," Superlattices Microstruct. **25**, 1251–1288 (1999).
[27]P. Dubos, H. Courtois, B. Pannetier, F. K. Wilhelm, A. D. Zaikin, and G. Schön, "Josephson critical current in a long mesoscopic S-N-S junction," Phys. Rev. B **63**, 064502 (2001).
[28]P. Virtanen and T. Heikkilä, "Thermoelectric effects in superconducting proximity structures," Appl. Phys. A **89**, 625 (2007).
[29]M. Janssen, *Fluctuations and Localization in Mesoscopic Electron Systems* (World Scientific, 2001).
[30]G. R. Stewart, "Measurement of low-temperature specific heat," Rev. Sci. Instrum. **54**, 1–11 (1983).
[31]C. N. Singman, "Atomic volume and allotropy of the elements," J. Chem. Educ. **61**, 137 (1984).
[32]P. A. Beck and H. Claus, "Density of states information from low temperature specific heat measurements," J. Res. Natl. Bur. Stand. A **74A**, 449–454 (1970).